contribute equally to both of the degenerate lowest singlet states.

Amusingly, combining these two bent units in a planar model for **1** nearly restores the degeneracy (now fourfold) of the lowest singlet state, and causes essentially no change in the energy of the lowest singlet from that in the bent diyne model, in spite of the fact that there is a 0.18 eV difference in energy between the HOMO and SHOMO, according to CNDO/S. The lowest singlet state is composed of two-thirds of the configuration involving transfer of an electron from the HOMO (antibonding combination of in-plane diyne HOMOs) to the third vacant orbital (antibonding combination of out-of-plane diyne LUMOs) and one-third of the configuration involving transfer of an electron from the fourth occupied MO (bonding combination of in-plane diyne HOMOs) to the SLUMO (bonding combination of out-of-plane diyne LUMOs). The second, third, and fourth excited singlets are similar, involving a combination of transitions from in-plane occupied to out-of-plane vacant orbitals, or out-of-plane occupied to in-plane vacant orbitals. The multiconfiguration nature of the excited states results in clever masking by the molecule of the significant orbital energy changes which occur.

Thus, ultraviolet absorption spectroscopy appears not to be a particularly sensitive probe of the type of electronic interactions studied here, whereas photoelectron spectroscopy reveals significant interactions.

Acknowledgment. We wish to thank the National Science Foundation for financial support of this research. We also wish to thank Frank Fronczek for assistance with the calculations, and Michael Squillacote for low-temperature NMR measurements.

References and Notes

(1) (a) Louisiana State University. (b) Camille and Henry Dreyfus Teacher–Scholar Grant Recipient, 1972–1977; Alfred P. Sloan Foundation Research Fellow, 1975–1977. (c) University of California. (d) University of Nevada.
(2) L. T. Scott and G. J. DeCicco, *Tetrahedron Lett.*, 2663 (1976).
(3) R. Weiss, Ph.D. Dissertation, University of California, Los Angeles, Calif., 1976.
(4) E. Kloster-Jensen and J. Wirz, *Helv. Chim. Acta*, **58**, 162 (1975).
(5) G. Bieri, E. Heilbronner, E. Kloster-Jensen, A. Schmelzer, and J. Wirz, *Helv. Chim. Acta*, **57**, 1265 (1974).
(6) The photoelectron spectrum was recorded on a Perkin-Elmer PS-18 photoelectron spectrometer with an He(I) source, using xenon and argon as calibration standards.
(7) (a) F. Brogli, E. Heilbronner, V. Hornung, and E. Kloster-Jensen, *Helv. Chim. Acta*, **56**, 2171 (1973); (b) E. Heilbronner, T. B. Jones, and J. P. Maier, *ibid.*, **60**, 1697 (1977).
(8) P. Masclet, D. Grosjean, G. Mouvier, and J. Dubois, *J. Electron Spectrosc. Relat. Phenom.*, **2**, 225 (1973).
(9) P. Carlier, J. E. Dubois, P. Masclet, and G. Mouvier, *J. Electron Spectrosc. Relat. Phenom.*, **7**, 55 (1975), report a value of 9.05 eV for this IP.
(10) F. Sondheimer, Y. Amiel, and R. Wolovsky, *J. Am. Chem. Soc.*, **79**, 6263 (1957).
(11) H. Schmidt, A. Schweig, and A. Krebs, *Tetrahedron Lett.*, 1471 (1974).
(12) STO-3G calculations used Gaussian 70, QCPE No. 236, by W. J. Hehre, W. A. Lathan, R. Ditchfield, M. D. Newton, and J. A. Pople, and the STO-3G basis set described by W. J. Hehre, R. F. Stewart, and J. A. Pople, *J. Chem. Phys.*, **51**, 2657 (1969).
(13) D. J. Cram, N. L. Allinger, and H. Steinberg, *J. Am. Chem. Soc.*, **76**, 6132 (1954).
(14) P. D. Mollere and K. N. Houk, *J. Am. Chem. Soc.*, **99**, 3226 (1977); E. J. McAlduff and K. N. Houk, *Can. J. Chem.*, **55**, 318 (1977); L. N. Domelsmith, K. N. Houk, J. W. Timberlake, and S. Szilagyi, *Chem. Phys. Lett.*, **48**, 471 (1977); L. N. Domelsmith, K. N. Houk, R. A. Snow, and L. A. Paquette, *J. Am. Chem. Soc.*, in press.
(15) M. D. Gordon, T. Fukunaga, and H. E. Simmons, *J. Am. Chem. Soc.*, **98**, 8401 (1976).
(16) J. Del. Bene and H. H. Jaffé, *J. Chem. Phys.*, **48**, 1807, 4050 (1968); **49**, 1221 (1968); **50**, 563 (1969).

Proton Magnetic Resonance and Conformational Energy Calculations of Repeat Peptides of Tropoelastin. The Hexapeptide

Dan W. Urry,* Md. Abu Khaled, V. Renugopalakrishnan, and Rao S. Rapaka

Contribution from the Laboratory of Molecular Biophysics and the Cardiovascular Research and Training Center, University of Alabama Medical Center, Birmingham, Alabama 35294. *Received May 13, 1977*

Abstract: Detailed proton magnetic resonance data, obtained in chloroform–dimethyl sulfoxide solutions, are reported and utilized to derive a static approximation to the conformation of the repeat hexapeptide of tropoelastin, HCO-L-Ala$_1$-L-Pro$_2$-Gly$_3$-L-Val$_4$-Gly$_5$-L-Val$_6$-OMe. The experimental information includes data and analyses of all of the αCH–NH and the valyl αCH–βCH coupling constants allowing estimates of five ϕ and two χ torsion angles, of temperature dependence of peptide NH chemical shift providing information on secondary structure, and of nuclear Overhauser enhancement data allowing estimates of two ψ torsion angles. The secondary structure and torsion angle data are self-consistent giving rise to a satisfactory static model. Conformational energy calculations in vacuo are also reported for the hexapeptide which describe two conformational states one of which compares favorably with the experimentally derived conformation. Adding to the static model a Val$_{6,i-1}$ residue preceding the hexapeptide and fixing the ϕ and ψ angles of both Val$_6$ residues at the theoretically derived values allows formation of a 23-atom hydrogen-bonded ring which had previously been deduced in solution for the polyhexapeptide.

Introduction

Tropoelastin, the precursor protein of the biological elastin fiber, has been shown to contain three repeating peptide sequences: a tetrapeptide (L-Val$_1$-L-Pro$_2$-Gly$_3$-Gly$_4$)$_n$, a pentapeptide (L-Val$_1$-L-Pro$_2$-Gly$_3$-L-Val$_4$-Gly$_5$)$_n$, and a hexapeptide (L-Ala$_1$-L-Pro$_2$-Gly$_3$-L-Val$_4$-Gly$_5$-L-Val$_6$)$_n$.[1,2] Previous spectroscopic studies on the hexapeptide of tropoelastin, using primarily the methods of proton and carbon-13 magnetic resonance, have resulted in proposed intramolecular hydrogen bonds.[3,4] These hydrogen bonds are Ala$_1$ C–O···HN Val$_4$, Gly$_3$ NH···O–C Gly$_5$, and a weaker interaction, Gly$_3$ C–O···HN Gly$_5$. This description of preferred secondary structure falls short of a desired description which would include specification of all of the αCH–NH (ϕ), the αCH–C′ (ψ), and the αCH–

0002-7863/78/1500-0696$01.00/0

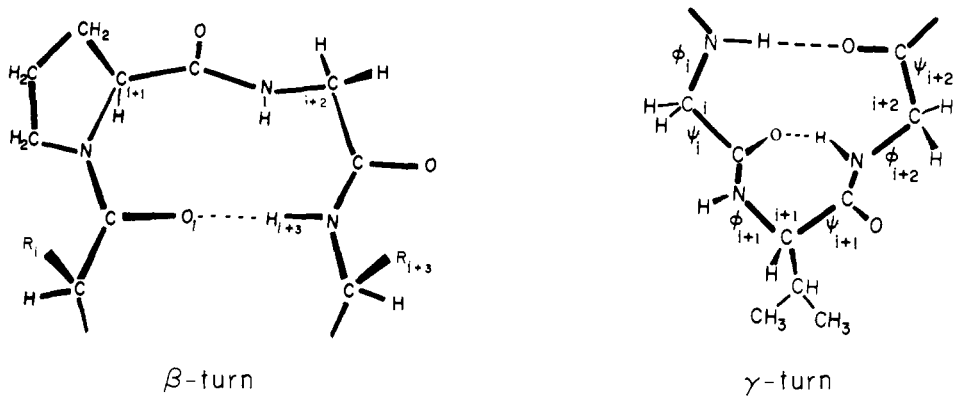

Figure 1. Two major secondary structural features of the repeat peptides of elastin. A. β turn showing a 10-atom hydrogen bonded ring. B. γ turn showing an 11-atom hydrogen bonded ring and the more flexible and acute 7-atom hydrogen bonded ring.

βCH (χ) torsion angles. Up until now, torsion angle information has been sufficiently fragmentary not to warrant attempts at detailed analysis. This has been due to the presence of the Gly_3 and Gly_5 residues and the lack of apparent ABX spin patterns for the αCH_2 protons. Recently we have found, however, that in the presence of sufficient chloroform, ABX spin patterns required to evaluate ϕ_3 and ϕ_5 are observed for these residues. Even with the limitations of a Karplus-like equation, this allows for a useful delineation of five of the six ϕ torsion angles with the sixth being restricted as the prolyl residue. Also recent developments in the utilization of the nuclear Overhauser effect make it possible to estimate values for ψ_i when the α proton, H_i^{α}, is at a distance of 3 Å or less from the peptide NH proton of residue $i + 1$.[5] With the constraints of three intramolecular hydrogen bonds and with restrictions placed on all six ϕ and several ψ torsion angles, construction of a Kendrew wire model containing the experimentally derived constraints allows estimates of all ψ torsion angles with the exception of ψ_1 and ψ_6.

Whether the ϕ and ψ angles derived in this manner are reasonable can be assessed, and the angles can be improved, by conformational energy calculations starting with the experimentally determined hydrogen bonding constraints as was successfully done for the valinomycin-K^+ complex[6] where proton magnetic resonance and conformational energy derived atomic coordinates were several years later shown to be correct to within less than 0.5 Å by x-ray crystallographic analysis.[7]

Theoretical conformational energy calculations on the related tetrapeptide, *t*-Boc-Val_1-Pro_2-Gly_3-Gly_4-OMe,[8] and pentapeptide, HCO-Val_1-Pro_2-Gly_3-Val_4-Gly_5-OMe,[9,10] a priori without experimentally derived constraints, have found the lowest energy conformations to have the same secondary structure as derived by means of nuclear magnetic resonance studies in solution and to have ϕ, ψ, and χ torsion angles which correspond reasonably well with those derived by the use of proton magnetic resonance to approximate ϕ and χ and by the use of a Dreiding model to add values for the ψ torsion angles. The apparent detailed success of the in vacuo calculations may be due in part to the low-polarity solvent used in the solution studies and in part to the peptides under study which, while exhibiting preferred conformation, show little cooperativity with the two major secondary structural features being largely independent of each other. Both the β turn (see Figure 1A), involving the ten-atom hydrogen-bonded ring, $residue_1$ C-O···HN $residue_4$ with Pro_2 and Gly_3 at the corners, and the γ turn (see Figure 1B), involving the 11-atom hydrogen-bonded ring, Gly_3 NH···O-C Gly_5, in the sequence Gly Val-Gly, have been shown to occur as independent conformational features.[11,12]

In the present effort, therefore, the combined approaches of proton magnetic resonance in chloroform, with the aid of a Kendrew model, and of conformational energy analyses are reported on the repeat hexapeptide of tropoelastin with the longer range goal of deriving atomic coordinates of the polyhexapeptide which would be useful in analyzing x-ray diffraction powder and fiber patterns. The purpose is to understand the role of the polyhexapeptide of tropoelastin in the function and pathology of biological elastic fibers. Of specific interest is the elastic fiber of vascular wall which is a primary site of two of the three major degenerative changes, the two being calcification and lipid deposition.

Experimental Section

The hexapeptide of elastin, *N*-formyl Ala_1-Pro_2-Gly_3-Val_4-Gly_5-Val_6-OMe, was synthesized in this laboratory.[4] To achieve an adequate molecularly dispersed solution (0.01 M) of this compound in $CDCl_3$, 10% Me_2SO-d_6 by volume was added. In varying the concentration from 0.1 M to 0.01 M in $CDCl_3$ a small concentration effect was observed; however, varying the concentration over the same range in the presence of 10% Me_2SO-d_6 resulted in removal of the concentration dependence, thereby providing evidence for the absence of aggregation at 0.01 M concentrations in $CDCl_3$ with 10% Me_2SO-d_6. The ^1H NMR spectra were obtained on a Varian HR-220 spectrometer operating at 21 °C. Fifteen percent by volume C_6D_6 was later added in order to separate resonances and thereby to facilitate the spectral analysis of Gly_3 CH_2 and Gly_5 CH_2 protons (see Figure 2). Simulated spectra were obtained with the SS-100 computer system of the Varian HR-220 spectrometer by means of a Varian Data Machine spin simulation program.

All double resonance experiments were performed on a JEOL PS-100 spectrometer operating in the internal lock mode and equipped with a JEOL JNM VT-3B temperature controller. Nuclear Overhauser enhancement (NOE) of signal intensity was measured from the difference of the integrated signal areas, at least five times (see Figure 3), with and without the second field (f_2) at the resonance frequency of the signal of interest. As the level of the second field (f_2) also affects the observed intensities of all signals in the spectrum,[13] the signal area was integrated when f_2 was at the signal of interest and then compared with the area obtained when the same level of f_2 was offset to a region of the spectrum containing no absorption signal. In the control experiment dimethylformamide in $CDCl_3$ was used and f_2 was placed on both sides of the observed signal. The accuracy of the reported % NOE values is about ±2.5%.

The ϕ torsion angles of the Val and Ala residues were approximated from the experimentally derived coupling constant, $^3J_{\alpha CH\text{-}NH}$, by means of a Karplus-like expression[14] using the coefficients of Bystrov et al.,[15] i.e.

$$^3J_{\alpha CH\text{-}NH} = 9.4 \cos^2 \theta - 1.1 \cos \theta + 0.4 \quad (1)$$

where the ^1H NMR derived torsion angle, θ, is related to ϕ as shown in Table II for $\phi = 0$ to ± 180°. For the ϕ torsion angles of the glycyl residues again coefficients derived by Bystrov et al.[15] were used, i.e.,

$$^3J_{\alpha CH\text{-}NH} + {}^3J_{\alpha CH'\text{-}NH} = -9.8 \cos^2 \phi - 1.3 \cos \phi + 15.0 \quad (2)$$

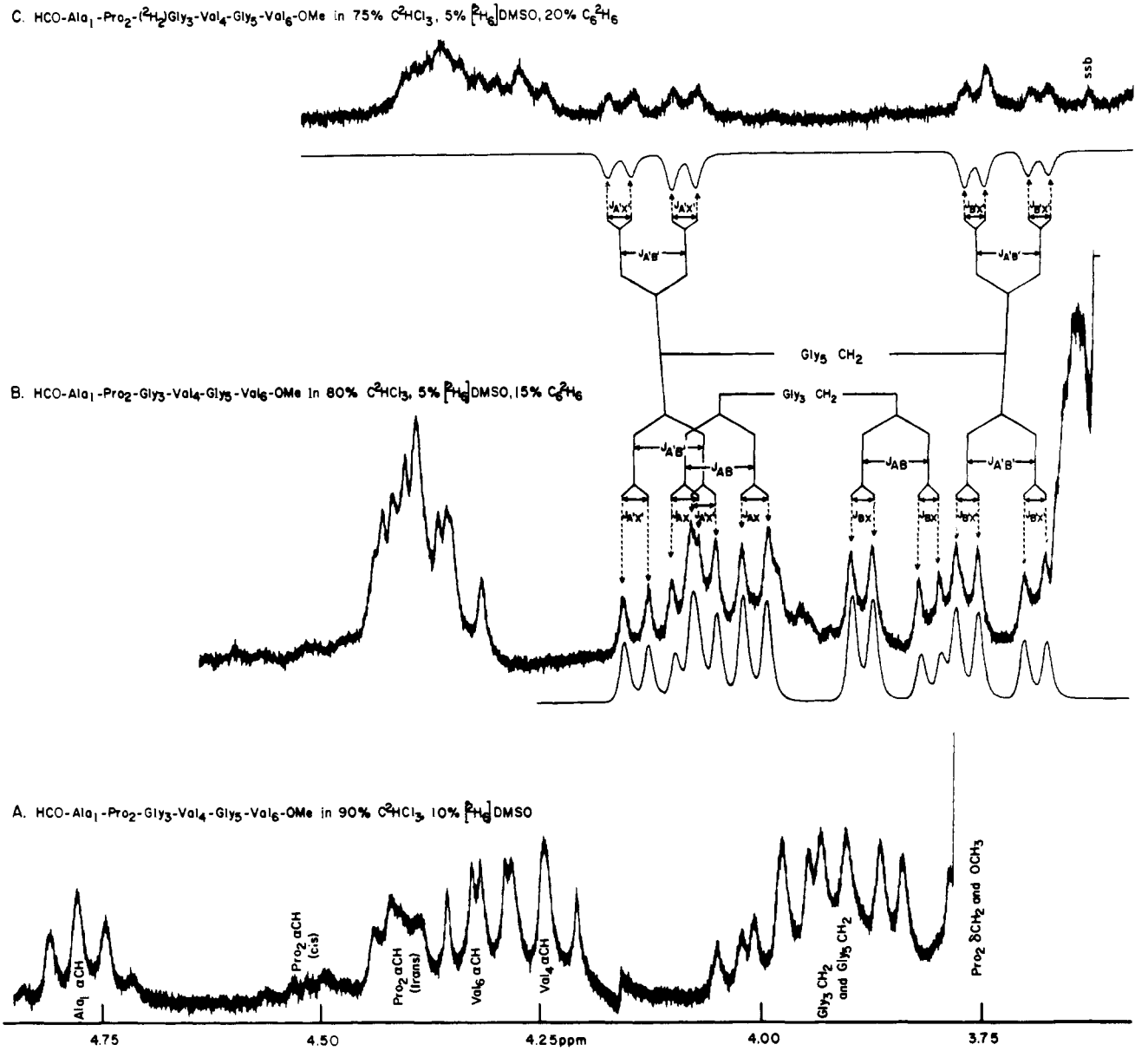

Figure 2. Proton magnetic resonance spectra of the αCH region taken at 220 MHz. A. HCO-Ala$_1$-Pro$_2$-Gly$_3$-Val$_4$-Gly$_5$-Val$_6$-OMe in $CDCl_3$–Me_2SO (9:1). B. HCO-Ala$_1$-Pro$_2$-Gly$_3$-Val$_4$-Gly$_5$-Val$_6$-OMe in $CDCl_3$–Me_2SO–C_6D_6 (80:5:15). The effect of benzene has been to separate the ABX patterns of the glycyl αCH_2 resonances from the other αCH resonances. Also included is the simulated spectrum for both glycyl αCH_2 ABX patterns. C. HCO-Ala$_1$-Pro$_2$-Gly$_3$(d_2)-Val$_4$-Gly$_5$-Val$_6$-OMe in $CDCl_3$–Me_2SO–C_6D_6 (75:5:20) showing only the ABX pattern of the Gly$_5$ αCH_2 resonances. This confirms the assignment and supports the spectral analysis. Note the simulated spectrum and compare to B.

where ϕ is directly used. The convention used for designating the angles ϕ, ψ, ω, and χ is that of the IUPAC-IUB Commission on Biochemical Nomenclature.[16]

Conformational Energy Calculations. In general the conformational energy calculations may be considered in terms of nine steps: (1) generation of the coordinates of the fully extended conformation with the valyl and alanyl side chains set in the trans configuration, (2) use of the partitioned potential energy method with appropriately derived potential energy parameters, (3) calculation of the potential energies on varying ϕ and ψ angles at 40° intervals but by first eliminating those conformations for which atom to atom distances are closer than the extreme limit, (4) calculation of potential energies in the low-energy region obtained in step 3 at 20° and then 10° intervals over the ±40° region, (5) rotation of side chains of low-energy conformation, which had been previously fixed in trans configuration, to find the energy profile and to place the side chain at its lowest energy, (6) carrying out energy minimization of the low-energy conformation by relaxing all backbone bond angles and allowing for peptide nonplanarity, (7) calculation and plotting of conformational energy maps for low-energy conformations, that is, while retaining the remainder of the molecule in its preferred conformation, ϕ_i and ψ_i of the ith residue are rotated to obtain the conformational energy map, (8) plotting minimum energy conformations, and (9) calculation of the expected coupling constants for the ϕ and χ bond rotations for the low-energy conformations and calculation of the expected % NOE values.

In developing the fully extended conformation of HCO-APGVGV-OMe the bond angles and lengths for the Val, Pro, and Gly residues and the methoxy groups were as used for the tetrapeptide[8] and pentapeptide.[9,10] For L-Ala an N-C^α-C′ bond angle of 110° and the C^α-C^β bond length of 1.53 Å[17] were used, and the C-H bond lengths were taken to be 1.09 Å. The *N*-formyl group was constructed using bond lengths of 1.32, 1.24, and 1.09 Å for the C′-N, C-O, and C-H bonds, respectively, and using bond angles of 125 and 115° for the angles N-C′-O and N-C′-H, respectively.[17]

Four energy terms were considered in the total conformational potential energy, E_T. These are van der Waals (E_{VDW}), electrostatic (E_{EL}), torsion (E_{TOR}), and hydrogen bond ($E_{H\text{-}B}$) energies, i.e.,

$$E_T = E_{VDW} + E_{EL} + E_{TOR} + E_{H\text{-}B} \quad (3)$$

The expression for the van der Waals energy utilized the Buckingham exponential-type potential function for the repulsive term and an r^{-6}

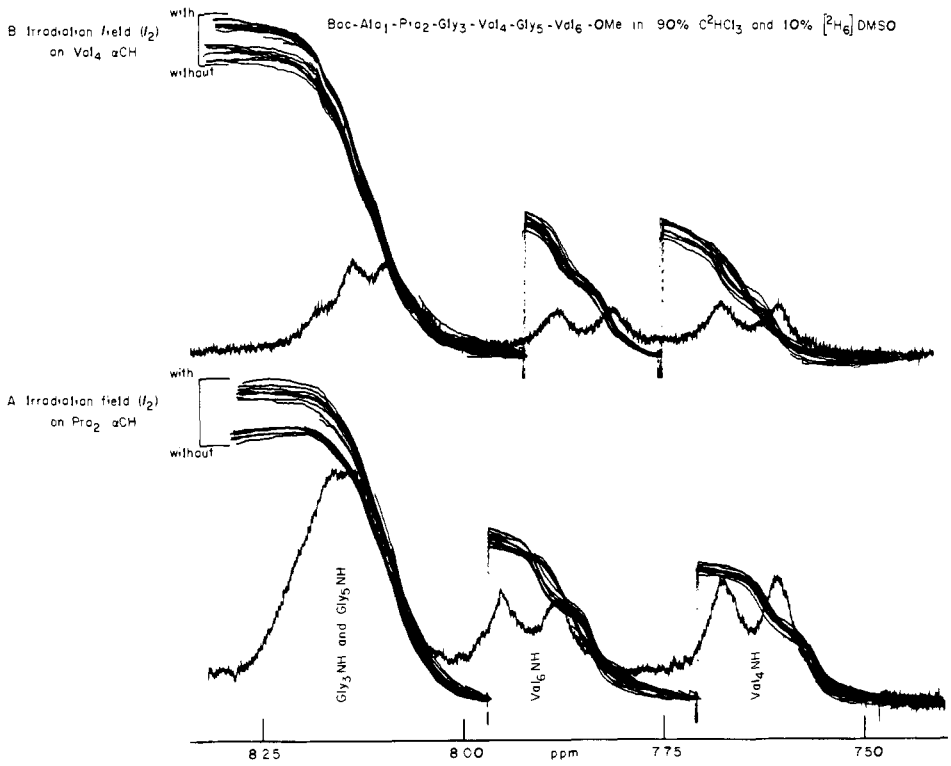

Figure 3. Nuclear Overhauser effects on the intensity of the peptide NH protons with irradiation of the Pro_2 αCH, A; and of the Val_4 αCH, B. See text for discussion.

attractive term with the parameters developed by Ramachandran and Sasisekharan.[18] For the electrostatic term Coulomb's expression was used with the dielectric constant taken as one and with monopole charges derived from ab initio minimal basis set (STO-3G) net charges for the formyl, L-alanyl, L-valyl, L-prolyl, glycyl, and OCH_3 moieties.[19-21] On assembling the net charges for the hexapeptide, care was taken to maintain electroneutrality of the peptide. The torsional energy was calculated using a threefold torsional potential with the barriers for rotation about the C^{α}–N bond taken as 0.6 kcal/mol and for rotation about the C^{α}–C′ bond taken as 0.2 kcal/mol.[22] Calculation of the hydrogen bond energies, which were not included in the ϕ, ψ map contours, utilized an empirical potential function for 7-, 10-, 11-, and 14-atom hydrogen-bonded rings which was derived by Ramachandran et al.[23] for the 10-atom hydrogen-bonded ring.

With ϕ_2 fixed at −60° due to the pyrrolidine ring there remain 11 backbone torsion angles, ϕ_1, ψ_1, ψ_2, ϕ_3, ψ_3, ϕ_4, ψ_4, ϕ_5, ψ_5, ϕ_6, and ψ_6, which are to be varied independently at steps of 40°. This means that 9^{11} conformations are considered but because of the imposition of the extreme limit criterion for close contact of atoms[18] only some odd million conformations are actually calculated. For example, in the case of an isolated valine residue there are nine angles (360/40) for ϕ and nine angles for ψ giving 9 × 9 or 81 conformations to be considered; however, the extreme limit criterion excludes all but five or six depending on the starting point for the 40° steps. This is, of course, what makes the search for a global minimum a tractable procedure. The low-energy conformations, obtained in the coarse search of 40° steps, are examined in finer detail, at 10° intervals, to position the minimum within the ±40° region. The side chains, of the low-energy conformations found in the above 10° search, are rotated to find their preferred orientation using a threefold torsional barrier of 2.8 kcal/mol.[22] With the side chains positioned at their energy minimum, an energy minimization procedure is carried out which allows relaxation of all backbone bond angles which, of course, also allows for a small amount of peptide nonplanarity. When ^{15}N enrichment is possible, the peptide nonplanarities, so obtained, can be compared with $^1J_{^1H\text{-}^{15}N}$ coupling constants which have been shown to be sensitive to nonplanarity of the peptide moiety.[24] This can, within a class of molecules, be used to check the reliability of the minimization procedure.

The ϕ, ψ maps calculated for the hexapeptide are obtained by starting with the molecule in a preferred conformation and holding the remainder of the molecule in the preferred conformation while varying one ϕ_i and ψ_i pair. With a map so obtained it becomes meaningful to calculate an expected coupling constant, $\langle J \rangle$. For the αCH–NH dihedral angle corresponding to the ϕ torsion angle we have the expected coupling constant $\langle {}^3J_{iC^{\alpha}H_i\text{-}NH_i} \rangle$ where

$$\langle {}^3J_{iC^{\alpha}H_i\text{-}NH_i} \rangle = \frac{\sum_{\phi_i} J_{\phi_i} e^{-\epsilon_{\phi i}/RT}}{\sum_{\phi_i} e^{-\epsilon_{\phi i}/RT}} \tag{4}$$

The values for J_{ϕ_i} are obtained from the equation of Bystrov et al. (see eq 1 and 2) for a given value of ϕ_i or for a set of low-energy ϕ_i. For the valyl side chain orientation we have

$$\langle {}^3J_{iC^{\alpha}H_i\text{-}C^{\beta}H_i} \rangle = \frac{\sum_{\chi_i} J_{\chi_i} e^{-\epsilon_{\chi i}/RT}}{\sum_{\chi_i} e^{-\epsilon_{\chi i}/RT}} \tag{5}$$

where the values for J_{χ_i} are obtained from the Abraham and McLauchlan equation,[25] i.e.,

$$J_{\chi_i} = \begin{cases} 10.5 \text{ Hz} \cos^2 |\chi_i| - 0.28 \text{ Hz for } |\chi_i| = 0\text{–}90 \\ 13.7 \text{ Hz} \cos^2 |\chi_i| - 0.28 \text{ Hz for } |\chi_i| = 90\text{–}180 \end{cases} \tag{6}$$

ϵ_{ϕ_i} and ϵ_{χ_i} are the energies for rotation of ϕ and χ, respectively, for the ith residue. The theoretically derived coupling constants can then be compared with the experimental values.

Results

Proton Magnetic Resonance. The proton magnetic resonance (^1H NMR) spectrum of the αCH region of HCO-Ala_1-Pro_2-Gly_3-Val_4-Gly_5-Val_6-OMe (APGVGV), shown in Figure 2A, was obtained in $CDCl_3$ to which Me_2SO-d_6 (10% by volume) was added to increase the solubility of the peptide. The αCH assignments of the Ala_1 and Pro_2 proton signals were easily made by observing their multiplet structure and were confirmed by double resonance experiments. The Val_4 and Val_6 assignments were made by utilizing our previous assignments in Me_2SO-d_6[4] and carrying out an Me_2SO to $CDCl_3$–Me_2SO-d_6 (9:1) solvent titration. Assignments of the

Table I. ^{1}H NMR Parameters of NF-APGVGV-OMe in a Solvent Mixture of $CDCl_3$-Me_2SO-d_6 (90:10 by Volume)

Parameters	L-Ala_1	L-Pro_2	Gly_3	Val_4	Gly_5	Val_6
Chemical shifts, ppm (±0.01)						
δ(NH)	8.26		8.46	7.71	8.33	8.36
δ(αCH)	4.77	4.41	4.06,[a] 3.88[a]	4.24	4.13,[a] 3.76[a]	4.31
δ(βCH)	1.27	*b*		*b*		*b*
δ(γCH)		*b*		0.91, 0.89		0.87
δ(δCH)		*c*				
Coupling constants, Hz (±0.1)						
^3J(αCH-NH)	7.3		6,[a] 5[a]	7.8	6,[a] 5.5[a]	8.5
^3J(αCH-βCH)	7.0	*d*		8.5		7.5
^3J(βCH-γCH)		*d*		7.0		7.0
^2J(αα)			−17.0		−17.0	
Temp coeff (Δδ/ΔT), ppm/°C						
Peptide NH	0.0091		0.0048	0.0039	0.0051	0.0086

[a] Values obtained by an ABX spin analysis in a solvent mixture of $CDCl_3$-Me_2SO-d_6-C_6D_6 (80:5:15). [b] Overlapped at 2.25–1.80 ppm. [c] Overlapped with OMe signal. [d] Not analyzed.

Table II. Nomogram of Possible Values of ϕ_i Derived from $^3J_{\alpha CH-NH}$ (—)[a] and Constrained Model (↓)

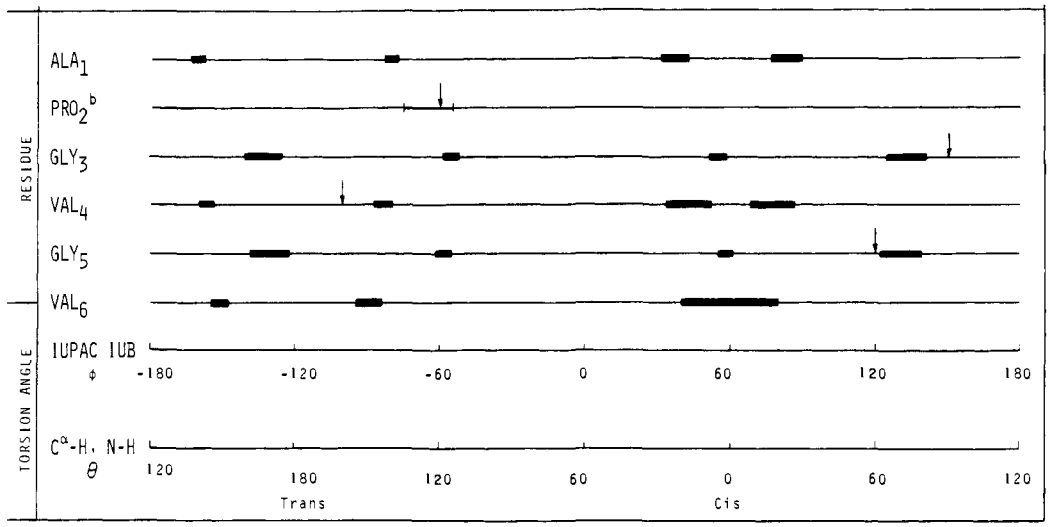

a) Using the Bystrov, et al. equations (15).
b) Usual range of ϕ for Pro is from −55° to −75° (36) with −60° chosen for Pro as residue i+1 in a β-turn (27).

Gly_3 and Gly_5 αCH_2 signals were achieved by comparing the spectrum of HCO-Ala_1-Pro_2-$Gly_3(d_2)$-Val_4-Gly_5-Val_6-OMe [APG(d_2)VGV] with that of APGVGV in a similar solvent mixture (see Figures 2B and 2C). The ABX spin systems of both glycine αCH_2 resonance patterns are apparent in Figure 2. In Figures 2B and 2C perdeuteriobenzene has been added in order to achieve separation of the resonances with the purpose of facilitating analysis. The Gly_3 αCH_2 protons are designated ABX and the Gly_5 αCH_2 protons are indicated by A′B′X′. With the $Gly_3(d_2)$ derivative, assignment of the glycine protons is unambiguous but this was also verified by double resonance. The glycine αCH_2 signals were analyzed as ABX spin systems using a spin simulation program and the simulated spectra are also included in Figures 2B and 2C. The values for the chemical shifts and coupling constants are listed in Table I.

The appearance of ABX spin patterns for both glycine methylene protons indicates formation of a constrained conformation presumably due to the intramolecular H-bond interaction.[8,26,27] Since temperature dependence of peptide NH protons provides information on such intramolecular interactions,[11,28,29] the temperature coefficients for all the NH protons of APGVGV in $CDCl_3$ were obtained and are also listed in Table I. Similar to the previous findings in other solvents,[11] the temperature dependence (Table I) shows the Gly_3 NH, Val_4 NH, and Gly_5 NH protons to be shielded from solvent by intramolecular interactions whereas the Ala_1 NH and Val_6 NH are essentially totally exposed to solvent. Of particular interest was the Gly_5 NH involvement which may give rise to a short-range interaction with Gly_3 C=O forming a seven-atom (C_7) ring structure similar to one which was found to occur within a γ turn.[12,30,31] A Kendrew model of the structure shows a close proximity of the Val_4 αCH and Gly_5 NH protons which might be expected to exhibit a nuclear Overhauser enhancement (NOE).[13] Therefore, NOE experiments were performed to evaluate the percent enhancement and proton proximity.[32] It was observed previously[33] in Me_2SO that, on saturation of the Pro_2 αCH by a second field (f_2), signal enhancement of the Gly_3 NH was obtained. This demonstrated the occurrence of a type II β turn.[33] A similar experiment was performed with this molecule, APGVGV, in the present solvent system to find a 16.5% NOE (see Figure 3A). On saturating the Val_4 αCH, a 9.5% NOE is obtained in the Gly_5 NH signal (see Figure 3B). Using the correlation[34] of NOE with the internuclear distance, r_{ij}, gives

$$\% \text{ NOE} = 100/kr_{ij}^6 \qquad (7)$$

where $k = 1.8 \times 10^{-2}$ Å^{-6} for the distance between two pro-

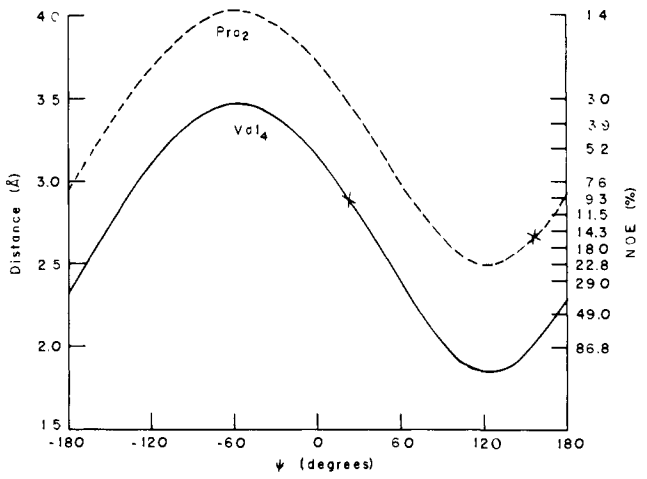

Figure 4. Plots of the distance in Å as a function of ψ for the Pro_2 αCH and Gly_3 NH protons, upper dotted curve, and for the Val_4 αCH and Gly_5 NH protons, lower solid curve. On the left hand ordinate are the corresponding % NOE values. The x on each curve correlates the experimental % NOE and the theoretically derived value for ψ.

tons.[35] With eq 6 distances corresponding to 16.5 and 9.5% are calculated to be 2.63 and 2.89 Å, respectively. As proposed by Leach et al.,[5] these values can be used to evaluate ψ_i. In the hexapeptide HCO-APGVGV-OMe in chloroform, efforts to evaluate ψ_i by this means are limited to the Pro_2 and Val_4 residues because the Ala_1 αCH has no corresponding NH proton in the Pro_2 residue, the Gly αCH_2 protons are overlapping with widely split ABX patterns making evaluation of NOE difficult, and the Val_6 αCH has no residue 7 NH with which to interact. Using the energy-minimized coordinates from the theoretical calculations for the atoms and bond systems involved, as discussed below, yields NOE derived values for ψ_2 of between +90° and +150° and for ψ_4 of either +25° or −140° (see Figure 4).

With the experimental αCH-NH coupling constants and utilizing the Bystrov et al.[15] equations (eq 1 and 2), the set of possible values for ϕ_i, included as expected ranges, are given in Table II. In the discussion these values will be systematically considered in combination with a Kendrew wire model containing flexible hydrogen bonding constraints to arrive at a static approximation to the solution conformation which will then be generalized to a more realistic description by considering theroetically expected, averaged coupling constants and % NOEs. This is achieved by considering the region of configuration space which contains conformations of a given class.

Conformational Energy Calculations. The in vacuo conformational energy calculations resulted in the finding of two classes of conformations. Considering conformations which differed by 10° in one torsional angle, conformation A contained 55 conformers and conformation B contained 42 conformers, this being the case when considering conformations up to 1.5 kcal/mol above the lowest energy conformer. The lowest energy conformer in each class is given in Figure 5. These two classes are most easily distinguished by the presence or absence of the 14-atom hydrogen-bonded ring involving the Ala_1 NH and the Val_4 C-O. The minimum energy of the two classes differs by 2.59 kcal/mol, when the hydrogen bonding energy is included, with conformation A being lower. Torsional angle maps, ϕ-ψ plots, where the remainder of the molecule is retained in its lowest energy conformation, are given in Figure 6 for conformation A. These are the types of maps which are then used to calculate the expected coupling constant and % NOE. The intent is to obtain a theoretical value that has greater significance for comparison with an experimental value which is most commonly the average of interconverting conformers in solution states. Conformers may differ, for example, simply by the value of a pair of torsion angles.

Realizing that small deviations in backbone geometry such as peptide nonplanarity[37] could, energetically, be more than compensated for by making other interactions within the peptide more favorable, a previously described[38] energy minimization procedure was carried out. This application to peptides utilized the Newton-Raphson method which had been employed by Boyd[39] for nonpeptide systems. Table III contains the values of the bond angle, τ, and of torsion angles ω, θ_N, and $\theta_{C'}$ which were obtained in deriving the conformers given in Figure 5. These angles are defined in footnotes to Table III. Rather than a τ of 109.5°, the values are seen to vary from 108° to 114°. The values for ω, which are 180° for entirely trans peptides, are seen to vary as much as 10° for peptides with NH moieties and as much as 18-20° for peptides containing the proline nitrogen. θ_N, also a measure of peptide nonplanarity, is zero for a planar peptide and is found to have values as high as 17° in the case of the Pro nitrogen but otherwise distorts up to about 10°. The values for $\theta_{C'}$ are, as expected,[37] found to be smaller.

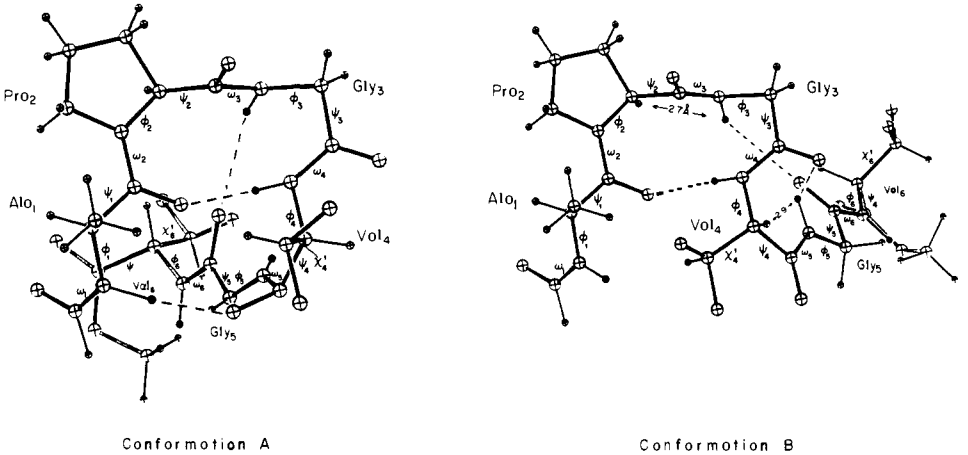

Figure 5. The lowest energy conformers in each of the two conformational states A and B. Conformational state A is typified by the presence of a 14-atom hydrogen bond between the residue$_1$ N-H and the residue$_4$ C-O. Conformational state B is typified by the absence of the 14-atom hydrogen bonded ring and the presence of a weak 7-atom hydrogen bonded ring. Both conformations contain the β turn with its 10-atom hydrogen bonded ring and the γ turn with its 11-atom hydrogen bonded ring. Also indicated on conformer B are the distances between the Pro_2 αCH and Gly_3 NH protons and between the Val_4 αCH and Gly_5 NH protons. The latter interaction, giving rise to a 9.5% NOE, is unique to conformational state B. In conformer A the Val_4 αCH-Gly_5 NH distance with a ψ_4 of −70 (see Table IV) would give rise to a % NOE which is at the limits of detectability.

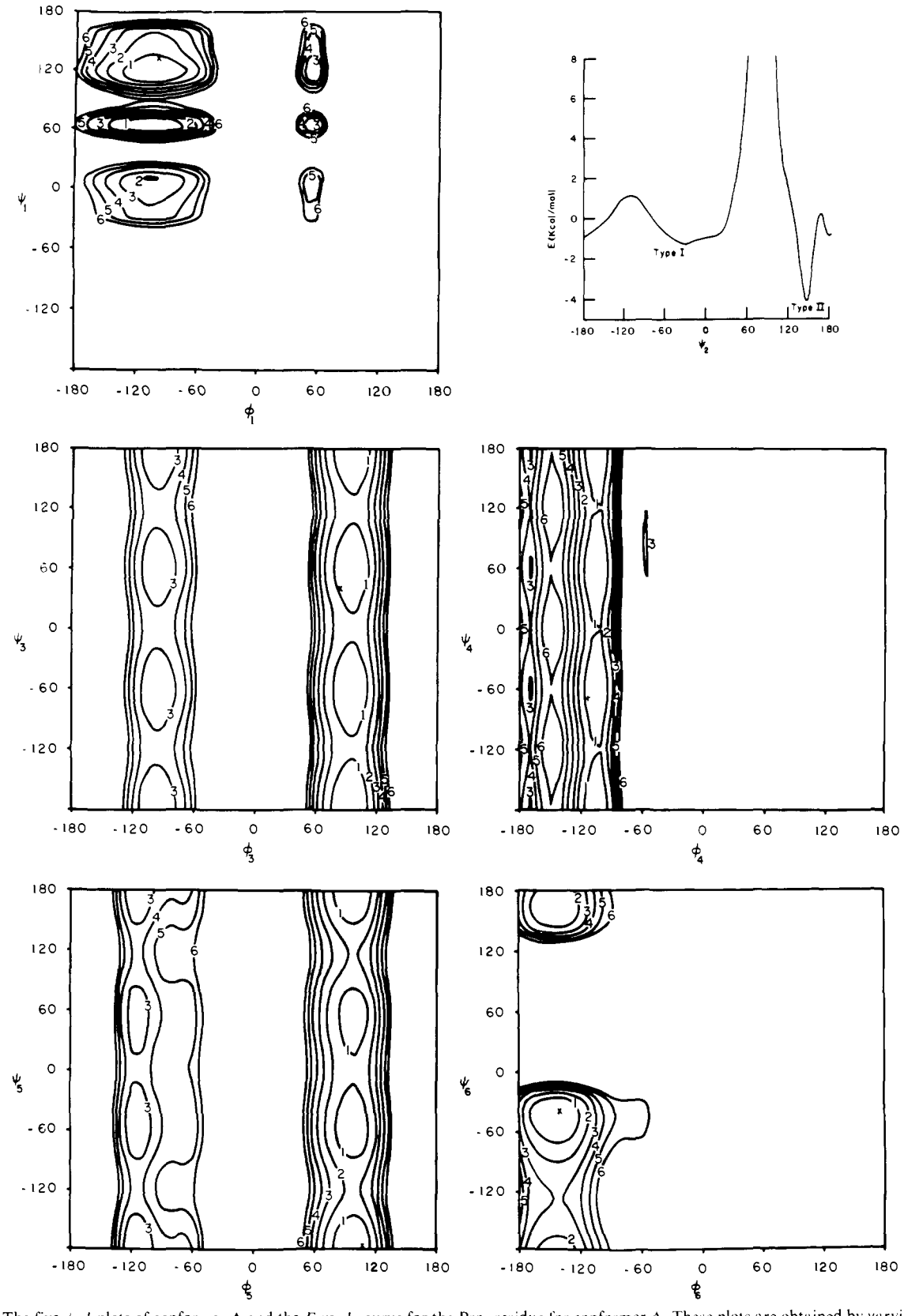

Figure 6. The five ϕ, ψ plots of conformer A and the E vs. ψ_2 curve for the Pro_2 residue for conformer A. These plots are obtained by varying a single ϕ, ψ pair while retaining the remainder of the molecule with the ϕ and ψ values listed in Table IV for conformer A. These maps and profile are then used to calculate the expected coupling constants and % NOE values for the conformational state.

Aside from high-resolution x-ray diffraction studies of peptides in the crystalline state, it has not, until recently, been possible to assess peptide nonplanarity in solution. Recently it has been shown that the $^1J_{^1H-^{15}N}$ coupling constant can be correlated with nonplanarity.[24,40] Analysis of the ^{15}N enriched tetrapeptide, Boc-Val-Pro-Gly-Gly-OMe, and the tripeptide, NAc-Gly-Val-Gly-OMe, results in values for $^1J_{^1H-^{15}N}$ which correspond satisfactorily with the nonplanarities obtained from theoretical calculations using the same methods as utilized here for the hexapeptide.[24] This provides for some confidence in the

Table III. Bond Angles τ[a] and Torsion Angles ω, θ_N, and $\theta_{C'}$[b] (deg) for Hexamer

	Conformation A				Conformation B			
	τ	$\lvert\omega\rvert$	$\lvert\theta_N\rvert$	$\lvert\theta_{C'}\rvert$	τ	$\lvert\omega\rvert$	$\lvert\theta_N\rvert$	$\lvert\theta_{C'}\rvert$
Ala_1	111	178	10	~0	111	179	9	~0
Pro_2	113	160	14	2	114	162	17	3
Gly_3	111	170	8	4	110	169	10	5
Val_4	114	177	9	7	115	175	8	4
Gly_5	108	170	10	6	110	175	11	5
Val_6	113	175	6	4	114	178	5	3

[a] Bond angle τ denotes $C_i'-C_i^\alpha-N_i$. [b] Torsion angles ω, θ_N, and $\theta_{C'}$ denote dihedral angles between planes $C_i^\alpha-C_i'-N_{i+1}$ and $C_i'-N_{i+1}-C_{i+1}^\alpha$, between planes $C_i'-N_{i+1}-C_{i+1}^\alpha$ and $C_i'-N_{i+1}-H_{i+1}$, and between planes $N_{i+1}-C_i'-C_i^\alpha$ and $N_{i+1}-C_i'-O_i$, respectively. Sense of rotation is in accordance with IUPAC–IUB convention.[16]

use of energy minimization.

Given the geometries of the Pro_2 and Val_4 residues, it is useful, following Leach et al.,[5] to calculate the distance between αCH_i and NH_{i+1} protons as a function of ψ_i. The result is shown in Figure 4 where the right-hand ordinate also contains the corresponding % NOE by means of eq 7. The important point in the result is that the proline residue has significantly different geometry requiring a separate curve. The small geometry changes, resulting from energy minimization of the L-Val_4 residue, show a small but discernible displacement from the curve which Leach et al.[5] calculated for an L-Ala residue. These curves will be useful in developing the static conformation (see below).

Discussion

Development of the Static Model. The hexapeptide was constructed using Kendrew wire models with torsional angles which could be locked once values were refined by the limited angles obtained from experiment. The initial constraints were two hydrogen bonds (Ala_1 C–O···HN-Val_4 and Gly_3 NH···O–C Gly_5 attached by flexible springs which when linear gave a 2.9 Å N to O distance), the Gly_5 NH and Gly_3 C–O were directed on the same side of the γ turn to approximate the experimental Gly_5 NH shielding, and ϕ_2 was taken as $-60°$ as the pyrrolidine ring allows a range of $-55°$ to $-75°$ for the ϕ of Pro with $-60°$ being found in the crystal with Pro as residue $i + 1$ of a β turn.[27,36]

With these constraints ϕ_3 was measured on the wire model to be 150°, which lies closest to the ^3J derived value near 130° (see Table II). ϕ_3 was then locked at 130°. Measurement of ϕ_4 gave a value of $-100°$, which is closest to the ^3J derived value near $-80°$, and ϕ_4 was locked at $-80°$. Measurement of ϕ_5 on the wire model gave a value of 120° making obvious the choice of 130° derived from ^3J (see Table II), and ϕ_5 was locked at 130°. Inspection of Table II shows graphically just how closely the initial wire model derived values approximated one of the four solutions from the Bystrov equation, which both makes the choice of a solution easy and gives confidence in it.

The next two values measurable on the above derived ^{1}H NMR-wire model which may be compared with experimentally derived values are the ψ_2 and ψ_4 torsion angles. The measured angle from the ^{1}H NMR-wire model for ψ_4 is 30° and the expected values (see Figure 4) from the NOE experiments (see Figure 3) are 25 and $-140°$. The correspondence of 30 and 25° is striking. The measured angle ψ_2 of 120° lies directly between the two values of 90 and 150° obtained from the NOE studies (see Figure 4). These values are surprisingly close for a static model. The value of ψ_2 derived from the theoretical calculation is 140°.

Stepping through the ^{1}H NMR analysis utilizing the wire model leads to a satisfactory description for residues 2, 3, 4, and 5 (see Figure 7). Residues 1 and 6 are outside of the hydrogen bonding constraints and no αCH_i–NH_{i+1} NOE values

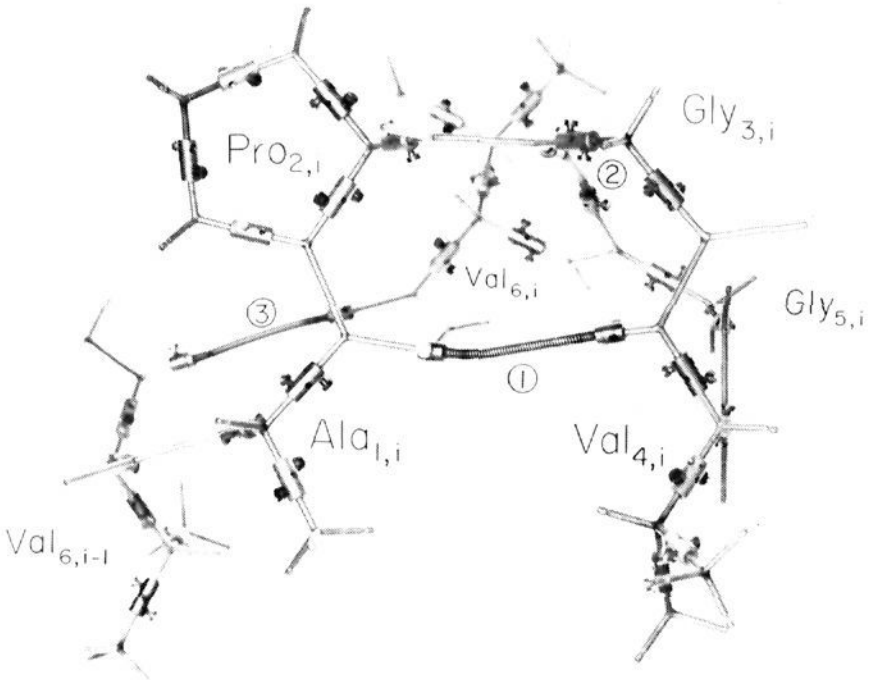

Figure 7. ^{1}H NMR-wire model of the hexapeptide conformation in which the Val_6 residue of the preceding repeat has been added and in which the $Val_{6,i-1}$ and $Val_{6,i}$ residues have been set with identical ϕ and ψ values derived by means of the theoretical calculations. The significant point is that the 23-atom hydrogen-bonded ring, proposed in the polyhexapeptide studies,[43,11] is formed. 1 indicates the hydrogen bond for the 10-atom ring (β turn), 2 indicates the hydrogen bond for the 11-atom ring (γ turn) and 3 indicates the hydrogen bond of the 23-atom ring.

are possible. The only experimental information for residues 1 and 6 is obtained from the values for ^3J. These possible values for ϕ_1 and ϕ_6, given in Table II, can, however, be compared with the theoretically derived values to arrive at a solution description with a reasonable level of confidence.

The ϕ and ψ values derived above for the Gly_3 and Gly_5 residues can be compared with ranges expected from the ^2J analysis of Barfield et al.[41] Both glycyl residues exhibit ^2J values of 17 Hz (see Table I and Figure 2). Using Figure 3 of Barfield et al.[41] for values of ϕ and ψ that correspond to given values of ^2J, it is seen that ϕ would be in the range of 50° to +130° and $-50°$ to $-130°$ and ψ would be in the ranges 0° to ±30°, +150° to +180°, and $-150°$ to $-180°$. As seen in Table IV, ϕ_3 and ϕ_5 are each given as 130° in accordance with ^2J; ψ_3 is $-40°$, about 20° outside the ^2J range, and ψ_5 is $-170°$, in the middle of the expected range. Accordingly the ^2J derived ranges are reasonably close to the values obtained in the static ^{1}H NMR-wire model.

Comparison of the ^{1}H NMR-Wire Model with the Lowest Energy Conformers in Conformational States A and B. On examination of the values in Table IV for the theoretically derived conformers A and B, it is seen in terms of torsion angles that the difference lies almost exclusively in the values for the Val_4 residue where $\phi_4^A = -110$ and $\psi_4^A = -70$, and $\phi_4^B = -60$ and $\psi_4^B = 30$. On comparison with the values for the ^{1}H NMR-wire model where $\phi_4 = -80$ and $\psi_4 = 25$, it is apparent

Table IV. Experimental and Theoretical Torsion Angles for HCO-Ala_1-Pro_2-Gly_3-Val_4-Gly_5-Val_6-OMe

Torsion angle	Ala_1		Pro_2		Gly_3		Val_4			Gly_5		Val_6		
	ϕ_1	ψ_1	ϕ_2	ψ_2	ϕ_3	ψ_3	ϕ_4	ψ_4	$\chi_4{}^{1c}$	ϕ_5	ψ_5	ϕ_6	ψ_6	$\chi_6{}^{1c}$
^{1}H NMR + wire model	−160[a]											−150[a]		
	−80		−60	120	130	−40	−80	25		130	−170	−90		
Conformer A[b]	−100	140	−60	140	80	40	−110	−70	−165	100	±180	−140	−40	±180
Conformer B[b]	−100	140	−60	140	80	40	−60	30	−165	150	±180	−140	−40	±180

[a] See Table II for the range of values when assuming a static structure. [b] The torsion angles are for the lowest energy conformer in each conformational state, i.e., for the conformers plotted in Figure 5. [c] The experimental values for $J_{\alpha CH\text{-}\beta CH}$ were 8.5 Hz for $\chi_4{}^1$ and 7.5 Hz for $\chi_6{}^1$ and the theoretically calculated expected values, $\langle J_{\alpha CH\text{-}\beta CH}\rangle$, were 8.6 and 7.9 Hz for conformation B and 8.5 and 7.9 Hz for conformation A whereas the torsion angles reported for A and B are for the lowest energy state.

that conformer B is most similar to the solution derived static model. This is consistent with the observation from the temperature dependence of peptide NH chemical shift studies (see Table I) where $d\delta/dT$ for the Ala_1 NH is 0.0091 ppm/deg, i.e., the most solvent exposed peptide NH. In conformer A the Ala_1 NH is hydrogen bonded whereas in conformer B the Ala_1 NH is exposed to solvent. Because both the Val_4 torsion angles and the hydrogen bonding data are in accord, one is compelled to take the view that the set of conformers referred to as conformation B best represents the solution conformation.

Significant differences, however, are observed between the torsion angles derived from the ^{1}H NMR-wire model for the Gly_3 residue and for those of conformer B (see Table IV). The source of the energy difference is apparent on examination of the conformational energy maps. The ϕ_3, ψ_3 plot for conformer B, not shown here, is similar to that given in Figure 6 for conformer A except that the allowed region between ϕ_3 +60 and +120 is broader such that a value of $\phi = +130$ is included within the lowest energy contour, and, of course, by the map in Figure 6 a ψ_3 of −40 for a given allowed value of ϕ is energetically the same as a ψ_3 of +40. As the ϕ, ψ maps contain all of the energy terms except the hydrogen bonding energy, the favoring of the plotted conformer B in Figure 5 is due to the calculated hydrogen bonding energy. The energy difference between the plotted conformer B in Figure 5 and the conformer which corresponds to the solution-derived model is 1.9 kcal/mol and may be due to limitations in calculating the hydrogen bonding energy.

One, of course, discusses static models not because we believe this to be the true situation in solution but because they are an essential, tractable step in achieving a solution description. While the hexapeptide of elastin as the monomer and as the high polymer is considerably more rigid in solution than the repeat pentapeptide, tetrapeptide, and their high polymers, it, nonetheless, is a dynamic structure. A means of accounting for this conformational mobility is to compare expected coupling constants and % NOE values which are calculated by considering the set of allowed regions in configuration space as outlined in the methods section. The theoretically derived expected coupling constants, $\langle {}^3J_{\alpha CH\text{-}NH}\rangle$, using eq 4 are 7.14 Hz for Ala_1, 5.5 Hz for Gly_3, 7.63 Hz for Val_4, 5.83 Hz for Gly_5, and 8.95 Hz for Val_6. These are to be compared with the experimental values (see Table I) of 7.3 Hz for Ala_1, (6 + 5)/2 Hz for Gly_3, 7.8 Hz for Val_4, (6 + 5.5)/2 Hz for Gly_5, and 8.5 Hz for Val_6. It is apparent that the correspondence between experiment and theory is improved by appropriately averaging over the allowed conformations. The correlation is equally good for calculating the expected % NOE, i.e.,

$$\langle \%\ \mathrm{NOE}\rangle = \frac{\sum_i (\%\ \mathrm{NOE})_i\, e^{-\epsilon_i/RT}}{\sum_i e^{-\epsilon_i/RT}} \qquad (8)$$

where for the Pro_2 αCH, Gly_3 NH interaction a value of 16.3% is calculated and a value of 16.5% was observed and for the Val_4 αCH, Gly_5 NH interaction a value of 8.0% is calculated and a value of 9.5% was observed.[42] The calculated and experimental values are within experimental error. Similarly for the valyl side chains using eq 5, the calculated values for the αCH-βCH coupling constants are 8.6 Hz for Val_4 and 7.9 Hz for Val_6 using the energy profiles for conformer B and the experimental values are 8.5 Hz for Val_4 and 7.5 Hz for Val_6. Therefore the degree of confidence with which one can view conformational state B as representative of the conformation of the hexapeptide in $CDCl_3$-Me_2SO (9:1) solution is significant.

Comparison with Other Elastin Repeat Peptides. In a similar conformational energy study on the tetrapeptide, Boc-Val_1-Pro_2-Gly_3-Gly_4-OMe, only the low-energy conformational state was found which contained both the 10-atom hydrogen bonded ring of the β turn and a 14-atom hydrogen bonded ring as in conformation A (see Figure 5), and this theoretical structure compared very well with the ^{1}H NMR derived conformational details in $CDCl_3$ solution.[8] In the solvents of methanol, dimethyl sulfoxide, and water (the latter at temperatures below 50 °C) only the 10-atom hydrogen bonded ring is apparent in the polytetrapeptide on the basis of peptide NH temperature dependence studies;[11,43] however, on raising the temperature above 50 °C in water, the Val_1 NH becomes shielded as when forming conformation A. Thus the data indicate that conformation A appears in water at elevated temperature for the polytetrapeptide and in $CDCl_3$ for the tetrapeptide.

In the conformational energy study of the pentapeptide, HCO-Val_1-Pro_2-Gly_3-Val_4-Gly_5-OMe, conformation B was found prior to bond and torsion angle energy minimization[9] but after minimization conformation A also appeared and did so as the lowest energy conformational state.[10] The ^{1}H NMR study in chloroform derives conformational detail entirely consistent with conformation A but not with conformation B. In other solvents, however, i.e., in water below 50 °C, in methanol, in dimethyl sulfoxide, and in trifluoroethanol, conformation B is favored for the polypentapeptide[44] whereas above 50 °C in water conformation A becomes favored.[11] Thus both conformations A and B are observed for the polypentapeptide depending on the solvent and temperature.

In the present study on the hexapeptide, while both conformations A and B were found in the conformational energy calculations, conformation A was the lowest energy conformation but conformation B was found in $CDCl_3$-Me_2SO solution. In the other solvents of water below 50 °C, methanol, and dimethyl sulfoxide, conformation B appears to be the preferred conformation for the polyhexapeptide[45,11] and, while there is a transition near 50 °C in water, the Ala_1 NH remains as the most solvent-exposed peptide NH and instead it is the Val_6 NH that becomes shielded to give hydrogen bonding between repeating hexameric units.[45,11]

The above synopsis of our studies on the conformations of the repeat peptides of elastin is for the purpose of noting that the conformations are solvent dependent and that both con-

formational states, A and B, appear to be involved in the case of the polytetra- and polypentapeptides. In the case of the polyhexapeptide, however, an additional hydrogen bond becomes involved between repeating units (proposed between units $i-1$ and i, i.e. $Val_{6,i-1}$ NH···O-C $Val_{6,i}$) and the point we wish to make here is that this 23-atom hydrogen-bonded ring forms with the values derived in the ^{1}H NMR-wire model and with the $Val_{6,i-1}$ and $Val_{6,i}$ residues locked in their conformational energy derived torsion angles as shown in Figure 7. Thus it would appear that the values derived here for the hexapeptide may be useful in achieving a description of the polyhexapeptide in the temperature precipitated aqueous state that gives an x-ray diffraction pattern[46] and that is considered to be most relevant to the biological state.[47] The temperature precipitated aqueous state of the polyhexapeptide, loosely referred to as the coacervate state, has been shown to be filamentous in negatively stained electron micrographs with periodicities similar to those of native elastin[48] and to have two sharp x-ray diffraction rings.[46]

Acknowledgment. This work was supported in part by the National Institutes of Health, Grant HL-11310.

References and Notes

(1) J. A. Foster, E. Bruenger, W. R. Gray, and L. B. Sandberg, *J. Biol. Chem.*, **248**, 2876 (1973).
(2) W. R. Gray, L. B. Sandberg, and J. A. Foster, *Nature (London)*, **246**, 461 (1973).
(3) D. W. Urry and T. Ohnishi, "Peptides, Polypeptides and Proteins", F. A. Bovey, M. Goodman, and N. Lotan, Ed., Wiley, New York, N.Y., 1974, pp 230–247.
(4) D. W. Urry, L. W. Mitchell, and T. Ohnishi, *Biochim. Biophys. Acta*, **393**, 296 (1975).
(5) S. J. Leach, G. Nemethy, and H. A. Scheraga, *Biochem. Biophys. Res. Commun.*, **75**, 207 (1977).
(6) D. F. Mayers and D. W. Urry, *J. Am. Chem. Soc.*, **94**, 77 (1972).
(7) K. Neupert-Laves and M. Dobler, *Helv. Chim. Acta*, **58**, 432 (1975).
(8) Md. Abu Khaled, V. Renugopalakrishnan, and D. W. Urry, *J. Am. Chem. Soc.*, **98**, 7547 (1976).
(9) V. Renugopalakrishnan and D. W. Urry, *Int. J. Quantum Chem.: Quantum Biol. Symp.*, **No. 3**, 13–19 (1976).
(10) V. Renugopalakrishnan, Md. A. Khaled, and D. W. Urry, *J. Chem. Soc., Perkin Trans. 2*, in press.
(11) D. W. Urry and M. M. Long, *CRC Crit. Rev. Biochem.*, **4**, 1–45 (1976).
(12) M. A. Khaled, D. W. Urry, and K. Okamoto, *Biochem. Biophys. Res. Commun.*, **72**, 162 (1976).
(13) W. von Philipsborn, *Angew. Chem.*, **10**, 472 (1971).
(14) M. Karplus, *J. Chem. Phys.*, **30**, 11 (1959).
(15) V. F. Bystrov, S. L. Portnova, T. A. Balashova, S. A. Kozmin, Y. D. Gavrilov, and V. A. Afanasev, *Pure Appl. Chem.*, **36**, 19 (1973).
(16) IUPAC–IUB Commission on Biochemical Nomenclature, *J. Mol. Biol.*, **52**, 1 (1970).
(17) L. E. Sutton, "Table of Interatomic Distances and Configuration in Molecules and Ions," *Chem. Soc., Spec. Publ.*, **No. 18** (1965).
(18) G. N. Ramachandran and V. Sasisekharan, *Adv. Protein Chem.*, **23**, 283 (1968).
(19) R. Rein, T. J. Swissler, V. Renugopalakrishnan, and G. R. Pack, "Conformation of Biological Molecules and Polymers", E. D. Bergmann and B. Pullman, Ed., Academic Press, New York, N.Y., 1973, p 761.
(20) V. Renugopalakrishnan and F. Jordan, in preparation.
(21) K. Morokuma and L. Pedersen, *J. Chem. Phys.*, **48**, 3275 (1968).
(22) R. A. Scott and H. A. Scheraga, *J. Chem. Phys.*, **45**, 2091 (1966).
(23) G. N. Ramachandran, R. Chandrasekharan, and R. Chidambaram, *Proc. Indian Acad. Sci., Sect. A*, **74**, 270 (1971).
(24) V. Renugopalakrishnan, M. A. Khaled, K. Okamoto, and D. W. Urry, *Int. J. Quantum Chem.: Quantum Biol. Symp.*, **4**, 97 (1977).
(25) R. J. Abraham and K. A. McLauchlan, *Mol. Phys.*, **5**, 513 (1963).
(26) L. G. Pease, C. M. Deber, and E. R. Blout, *J. Am. Chem. Soc.*, **95**, 260 (1973).
(27) T. Ueki, S. Bando, T. Ashida, and M. Kakudo, *Acta Crystallogr., Sect. B*, **27**, 2219 (1971).
(28) M. Ohnishi and D. W. Urry, *Biochem. Biophys. Res. Commun.*, **36**, 194 (1969).
(29) D. W. Urry and M. Ohnishi, "Spectroscopic Approaches to Bimolecular Conformation", D. W. Urry, Ed., American Medical Association Press, Chicago, Ill., 1970, pp 33–121.
(30) G. Nemethy and M. P. Printz, *Macromolecules*, **5**, 755 (1972).
(31) B. W. Mathews, *Macromolecules*, **5**, 818 (1972).
(32) W. A. Gibbons, D. Crepaux, J. Delayre, J. Dunand, G. Hajdukovic, and H. A. Wyssbrod, "Peptides: Chemistry, Structure and Biology", R. Walter and J. Meienhofer, Ed., Ann Arbor Science Publishers, Ann Arbor, Mich., 1975, pp 127–136.
(33) M. A. Khaled and D. W. Urry, *Biochem. Biophys. Res. Commun.*, **70**, 485 (1976).
(34) J. H. Noggle and R. E. Schirmer, "The Nuclear Overhauser Effect", Academic Press, New York, N.Y., 1971.
(35) R. A. Bell and J. K. Saunders, *Can. J. Chem.*, **48**, 1114 (1970).
(36) B. Pullman and A. Pullman, *Adv. Proton Chem.*, **28**, 248–526 (1974).
(37) G. N. Ramachandran, A. V. Lakshminarayanan, and A. S. Kolasker, *Biochim. Biophys. Acta*, **303**, 8 (1973).
(38) V. Renugopalakrishnan, M. Renugopalakrishnan, and B. Sarkar, *Int. J. Quantum Chem.: Quantum Biol. Symp.*, **No. 2**, 109 (1975).
(39) R. H. Boyd, *J. Chem. Phys.*, **49**, 2574 (1968).
(40) M. Llinas, W. J. Horsley, and M. P. Klein, *J. Am. Chem. Soc.*, **98**, 7554 (1976).
(41) M. Barfield, V. J. Hruby, and J.-P. Meraldi, *J. Am. Chem. Soc.*, **98**, 1308 (1976).
(42) As the values ϵ_i in eq 8 are the energies above the lowest energy conformation of a single low-energy basin, ϵ_i is always less than 1.5 kcal/mol and as a result the interconversion between the 42 conformers considered in the averaging process would be rapid relative to the rotational correlation times.
(43) D. W. Urry and T. Ohnishi, *Biopolymers*, **13**, 1223 (1974).
(44) D. W. Urry, L. W. Mitchell, T. Ohnishi, and M. M. Long, *J. Mol. Biol.*, **96**, 101 (1975).
(45) D. W. Urry, T. Ohnishi, M. M. Long, and L. W. Mitchell, *Int. J. Pept. Protein Res.*, 7, 367 (1975).
(46) D. W. Urry, M. Mammi, and L. Gotte, *Bull. Mol. Biol. Med.*, in press.
(47) D. W. Urry, *Perspect. Biol. Med.*, **21**, 265 (1978).
(48) D. Volpin, D. W. Urry, I. Pasquali-Ronchetti, and L. Gotte, *Micron*, 7, 193–198 (1976).